

g_J factor of metastable 5S_2 atomic oxygen using a time-of-flight, atomic-beam magnetic-resonance method

Tuncay İncesu,* Ahsanul Huq,[†] and Howard A. Shugart

Department of Physics and Materials and Molecular Research Division, Lawrence Berkeley Laboratory,
University of California, Berkeley, California 94720

(Received 12 August 1977; revised manuscript received 22 May 1978)

A time-of-flight, atomic-beam magnetic-resonance method was used to compare the g_J factor of $2p^3 3s^2 S_2$ atomic oxygen with the g_J factor of metastable 2^3S_1 atomic helium in magnetic fields of 3209 and 4228 G. The metastable oxygen and helium atoms were produced in a pulsed radio-frequency discharge source and after traversing the apparatus were detected by electron emission from a tungsten surface. By collecting data only in a given interval of the time-of-flight distribution the $O(^5S)$ and $He(^3S)$ states were isolated from other discharge products. From 158 pairs of resonances taken with four relative field and hairpin orientations the atomic magnetic g factor is $g_J(^5S_2, ^{16}O) = \mu_J/J = -2.0020910(10)$.

I. INTRODUCTION

The present measurement stems from an unexpected observation. When beam-source development studies were initiated to produce metastable $N(^6S_{5/2})$ atoms from dissociation of N_2 , a velocity-selected Stern-Gerlach deflection experiment showed two magnetic moment peaks at $4\mu_0$ and $2\mu_0$ rather than the expected three peaks at $5\mu_0$, $3\mu_0$, and $1\mu_0$. The cause of this discrepancy was traced to the presence of $O(^5S_2)$ metastable atoms made from O_2 which entered the gas-handling system from the atmosphere by permeating a short section of plastic tubing. Although this interference was easily eliminated, the strength of the $O(^5S_2)$ signal and the intrinsic interest in atomic oxygen as a constituent of the atmosphere and as a test case for multielectron atomic theory compelled the precision measurement reported here.

The ground-state configuration of atomic oxygen ($1s^2 2s^2 2p^4$) produces two metastable levels 1D_2 and 1S_0 above the 3P_2 ground state. These states have energies 1.97 and 4.18 eV and lifetimes ≈ 150 and ≈ 15 sec., respectively. Another state 5S_2 is the lowest quintet state of the configuration $1s^2 2s^2 2p^3 3s$ and lies 9.14 eV above the ground state.¹ Three independent lifetime measurements of $O(^5S_2)$ yielded 185 ± 10 ,² 170 ± 25 ,³ and 180 ± 5 μ sec,⁴ which are consistent with a theoretical calculation of 192 μ sec.⁵

Throughout this paper all g_J values will be quoted using the convention $g_J = \mu_J/J$. This convention is consistent with that used for nuclei and, therefore, provides a uniform convention for the sign of a g factor. The negative sign for the free electron ($g_e \approx -2$) indicates the magnetic moment and angular momentum point in opposite directions. In 1949 Kiess and Shortley, obtained the value $g_J(^5S_2, ^{16}O) = -1.999(2)$ (Ref. 6) from the Zeeman pattern of the visible spectral lines of oxygen.

Eighteen years later Brink observed oxygen in an atomic-beam apparatus and compared the resonant frequencies of 5S and 3P states to obtain $g_J(^5S_2, ^{16}O) = -1.97(5)$.⁷ In addition to using a mass-spectrometer detector, Brink observed from his source two spectral lines 3947 and 7774 Å that result from transitions which terminate in the 5S_2 state.

The magnetic moment of the comparison helium state used in the current measurement has a long history of study by many techniques. When the present experiment was in progress the best value of the $g_J(^3S_1, ^4He) = -2.00223735(60)$ was from a previous measurement in this laboratory.⁸ Recently, two new values have been published: $g_J(^3S_1, ^4He) = -2.00223755(20)$ (Ref. 9) from an optical pumping experiment and $g_J(^3S_1, ^4He) = -2.00223745(14)$ (Ref. 10) from an atomic-beam experiment.

In the absence of nuclear spin and neglecting terms quadratic in the magnetic field, the energy levels shown in Fig. 1 are given by the expression $W = -g_J \mu_0 m_J B$. When $\Delta m_J = \pm 1$ transitions are observed, the g -factor ratio

$$g_J(^5S_2, ^{16}O)/g_J(^3S_1, ^4He) = \nu(^{16}O)/\nu(^4He),$$

where the ν 's are resonant frequencies in a common magnetic field. Justification for neglecting possible terms quadratic in field rests partly on theoretical and partly on experimental evidence. The nonrelativistic interactions of an atom with the external magnetic field are separated into terms linear in field

$$W_{\text{mag}}^I = (e/2m)\vec{B} \cdot (\vec{L} - g\vec{S})$$

and quadratic in field,

$$W_{\text{mag}}^{II} = \frac{e^2 B^2}{8m} \sum r_i^2 \sin^2 \theta_i,$$

where r_i and θ_i are the polar coordinates of the i th

electron and $\theta=0$ is the direction of B .¹¹ Shifts quadratic in the field may arise from $W_{\text{mag}}^{\text{I}}$ in second-order perturbation theory:

$$\Delta E_2^{\text{I}} = \sum_{n \neq 2} \frac{\langle 2^3S_1 | W_{\text{mag}}^{\text{I}} | n \rangle \langle n | W_{\text{mag}}^{\text{I}} | 2^3S_1 \rangle}{E(2^3S_1) - E(n)}.$$

Since $W_{\text{mag}}^{\text{I}}$ has nonzero matrix elements only between states of the same L and S , any intermediate states must have n^3S_1 character. However, $\langle 2^3S_1 | W_{\text{mag}}^{\text{I}} | n^3S_1 \rangle$ matrix elements for $n \neq 2$ are zero since $W_{\text{mag}}^{\text{I}}$ is independent of space coordinates and the spatial portions of the wave functions are orthogonal. Third-order effects of $W_{\text{mag}}^{\text{I}}$ are zero for the same reason. Similar arguments also hold for oxygen. Thus in the nonrelativistic limit there are no quadratic field terms from $W_{\text{mag}}^{\text{I}}$ for the states considered. The second-order shifts from $\Delta E_2^{\text{II}} = \langle 2^3S_1 m | W_{\text{mag}}^{\text{II}} | 2^3S_1 m \rangle$ are nonzero but independent of m since $W_{\text{mag}}^{\text{II}}$ does not affect the spin portion of the wave functions.

Nonlinear relativistic effects may occur through the spin-spin interaction and relativistic corrections to the magnetic-interaction operator. Relativistic corrections which may remove the m degeneracy of absolute shifts can be expected to be given by $(Z\alpha)^2$ times the absolute shift of the levels:

$$\Delta E_{\text{rel}}^{\text{II}} \approx (Z\alpha)^2 \langle 2^3S_1 | \frac{e^2 B^2}{8m} \sum r_i^2 \sin^2 \theta_i | 2^3S_1 \rangle$$

$$\approx 2.4 \times 10^{-7} (\text{Hz/G}^2) B^2$$

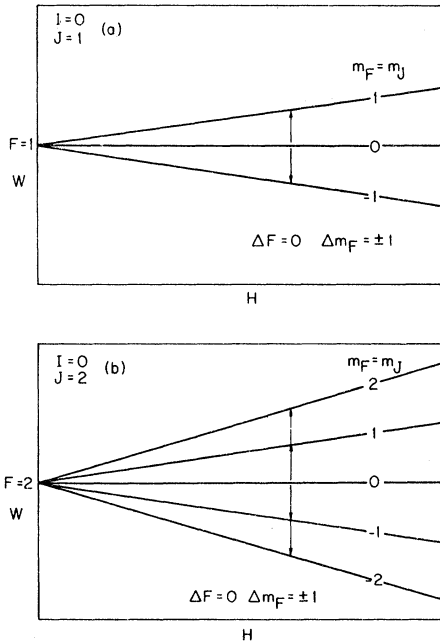


FIG. 1. Schematic of energy vs magnetic field for Zeeman levels and induced transitions (arrows) of (a) the 2^3S_1 state of helium and (b) the 5^3S_2 state of atomic oxygen. $F=I+J$.

using a hydrogenic approximation for the matrix element. At a field of 4000 G this corresponds to a shift of 4 Hz which is negligible in the current measurements.

Also since comparison of helium and oxygen resonances was made experimentally at two field values, certain limits may be placed on the quadratic dependence of the frequency. If both oxygen and helium resonant frequencies had a functional form

$$\nu = -g_J(\mu_0/h)B + bB^2,$$

then

$$\frac{\nu(\text{O})}{\nu(\text{He})} \approx \frac{g_J(\text{O})}{g_J(\text{He})} + [b(\text{He}) - b(\text{O})] \frac{B}{g_J(\text{He})\mu_0/h}.$$

Using ratios for $\nu(\text{O})/\nu(\text{He})$ of 0.999 926 8(5) at 3209 G and 0.999 927 0(5) at 4228 G,¹² the difference $b(\text{He}) - b(\text{O})$ should be smaller than 6×10^{-4} Hz/G². Within experimental error the two ratios are essentially equal, and, therefore, furnish no indication of a finite difference of the two b coefficients.

II. EXPERIMENT AND PROCEDURE

The atomic-beam apparatus employed in this work has been described previously.^{12,13} Modifications to the beam geometry shown in Fig. 2 permit the observation of both helium and oxygen resonances. In the A magnet the undeflected $m_J=0$ state is selected and passes through the C -magnet transition region. If no transition from this state occurs, the atoms strike a stop wire. On the other hand, if in the rf transition region the $m_J=0$ atoms make a transition either to $m_J = \pm 1$ or ± 2 , the B magnet deflects them to the side of the stop wire; and the atoms are counted by the Auger electron detector. This arrangement has the following advantages: (a) both the unknown and the calibration atoms have the same trajectory through the radio-frequency region; (b) flop-in resonances are observed with low, off-resonance background, i.e., the signal increases as the frequency approaches the resonant condition; (c) single quantum, $\Delta m_J = \pm 1$ resonances are detected in integral J atoms; and

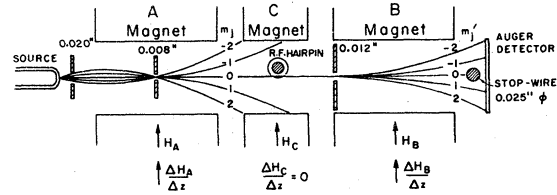


FIG. 2. Trajectory geometry and field configurations of the atomic-beam apparatus used in the oxygen g_J measurement. The distance from the source to the detector is about 2.5 m.

(d) the method is independent of the differences in deflection characteristics of the two species.

Both ³S₁ helium and ⁵S₂ oxygen were produced in a pulsed 50-MHz radio-frequency discharge tube. The active region of the discharge tube, 22 cm long and 0.8 cm in diameter, was bent into a U shape. A slit 0.005 in. wide and 0.160 in. high in the convex side allowed escape of the metastable beam. The radio frequency through the tube was pulsed on for 40 μsec about 150 times per second. This procedure permitted the time of flight to the detector to be used as a discriminator against photons, high-velocity atomic states, and low-velocity molecular states. The cold tungsten cathode surface of a Bendix magnetic electron multiplier emits electrons only when struck by sufficiently excited atoms and thus further discriminates against ground-state atoms and molecules. Any charged particles in the beam are deflected from the beam by the various apparatus's magnetic fields.

Magnetic field stability and homogenization in the C-magnet region were achieved by using two Klein-Phelps-type nuclear-magnetic-resonance (NMR) systems.¹⁴ One field-modulated system locked the C field to a particular value while a second frequency-modulated system allowed mapping vertically and horizontally along the beam. The first probe was fixed in position about 2 in. below the beam while the second probe was attached to the movable radio-frequency hairpin structure. By iterating a procedure of mapping the field and setting correction currents in eight shim coils,¹⁵ it was possible to reduce the inhomogeneity along a 2-in. length of the beam from 60 ppm to less than 1 ppm.

Radio frequency for inducing transitions was generated by an X-13 reflex klystron oscillator which was locked to harmonics of a HP 5105A frequency synthesizer. The output of the oscillator passes through a traveling-wave tube amplifier and power leveler before arriving at the 50-Ω terminated hairpin structure (see Ref. 16) where transitions in the beam are induced. The frequency was generated and measured to at least 1 part in 10⁸ and was based upon the atomic time scale of station WWVB at 60 kHz. The two frequencies for helium and oxygen at 3209 G were 8990.3 and 8989.6 MHz, while at 4228 G, they were about 11 845.5 and 11 844.7 MHz, respectively. These pairs of frequencies were sufficiently close together so the klystron could be tuned from one to the other by changing only the repeller voltage.

An on-line PDP-11 computer controlled the timing, apparatus parameters, time of flight, and resonance data collection for the experiment. During data taking with 40 μsec/channel and a 2.5-

m-long apparatus, the time-of-flight spectrum corresponding to the ⁵S₂ state of oxygen falls between the 6th and 30th channels, while most of the ³S₁ helium atoms fall between the 14th and 35th channels. With this data-collection arrangement the inverse relation between observed linewidth and traverse time in the radio-frequency region was easily demonstrated. Figure 3 shows a sample ⁵S₂ oxygen time-of-flight spectrum. For resonance data collection we used only those atoms which arrived at the detector between channel 10 and channel 35, since this range included most of the slower ⁵S₂ oxygen atoms and the entire ³S₁ helium peak. Alternately, the helium and oxygen resonances were scanned and recorded at 20 discrete frequencies. Adequate data were collected in 2 or 3 min on helium and in 10 to 15 min on oxygen. Usually six oxygen resonances imbedded between seven helium resonances were taken before altering the experimental conditions.

III. DATA ANALYSIS

In data collection and searching for systematic effects 372 individual helium and oxygen resonances were collected and fitted by least-squares methods to a Lorentzian line shape with a constant background. The resonance amplitude, peak frequency, and width, as well as the background, were determined. Figures 4 and 5 show examples of fitted oxygen and helium resonances. All resonances used to determine optimum rf powers were discarded, and only five other oxygen resonances

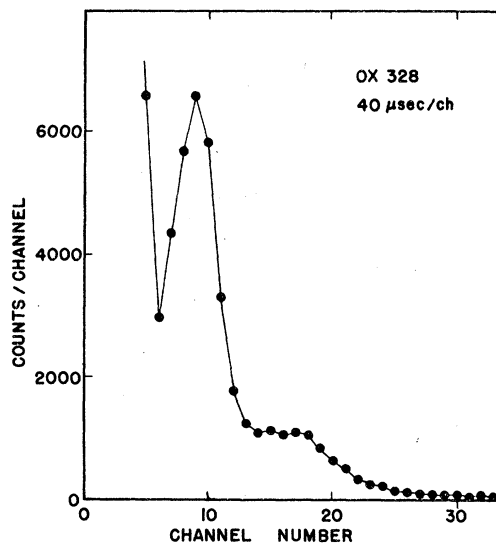


FIG. 3. Time-of-flight distribution of metastable dissociation fragments from O₂. Data-collection time was 10 min. The peaks between channels 6 and 30 correspond to ⁵S₂ atoms.

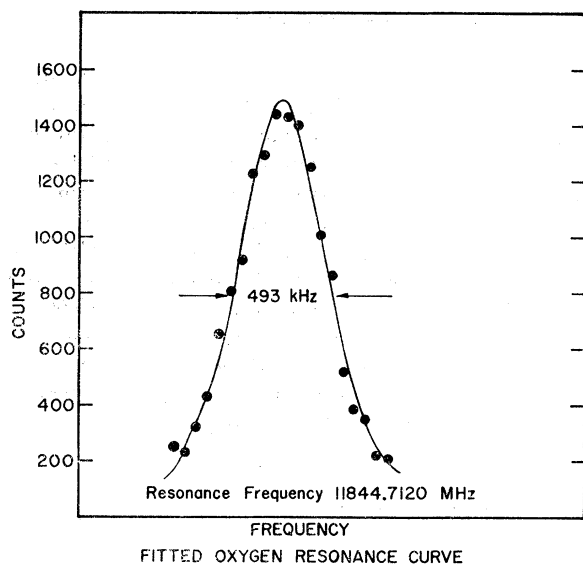


FIG. 4. Least-squares fit to an oxygen 5S_2 resonance curve. Data-collection time was 10 min.

were eliminated for various experimental reasons. In an effort to discover possible systematic effects, the remaining data were divided into two groups, one corresponding to a field of 4228 G and the other to a field of 3209 G. Each of these groups were split into four subgroups according to the four possible orientations of the C field and hairpin [each may be N (normal) or R (reversed)]. Finally these four subgroups were further divided into three smaller groups each having a different hairpin position. The ratio $g_J(^5S_2, ^{16}O)/g_J(^3S_1, ^4He)$ was

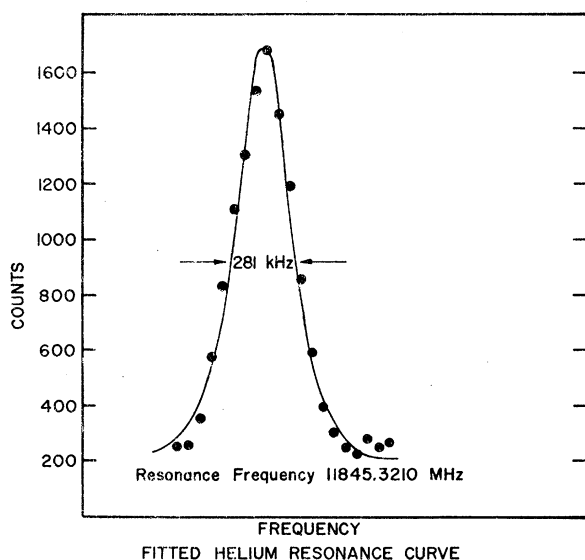


FIG. 5. Least-squares fit to a 3S_1 helium resonance curve. Data-collection time was 2 min.

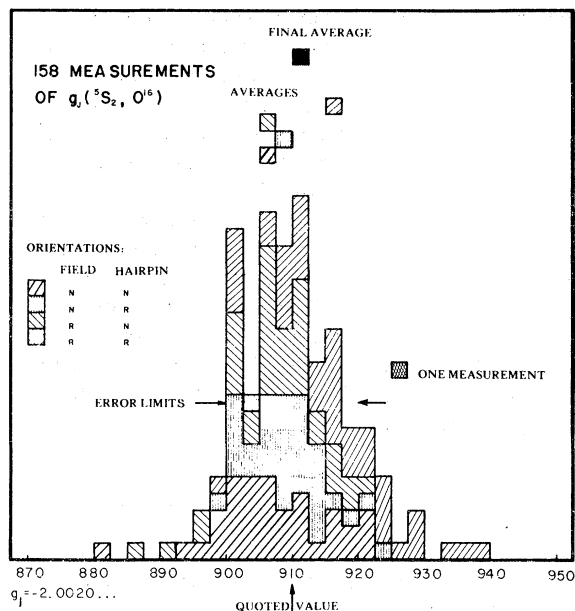


FIG. 6. Histogram of all oxygen 5S_2 g_J determinations. "N" and "R" refer to normal and reverse orientations of the C field or of the rf hairpin.

computed for every oxygen resonance frequency using the average of the two helium resonance frequencies taken just before and immediately after the oxygen resonance. The average value for each of the groups and subgroups provided an indication of the degree of systematic effects and allowed correction for the Millman effect which arises from variation of the rf field direction in the transition region.¹⁷

IV. RESULTS AND DISCUSSION

A summary of 158 measurements for the oxygen 5S_2 g_J is given in the histogram of Fig. 6. Above the histogram are indications of individual averages for the four field and hairpin orientations as well as the final average. From this analysis we find

$$g_J(^5S_2, ^{16}O)/g_J(^3S_1, ^4He) = 0.999\,926\,9(4).$$

When this result is combined with the 3S_1 helium g_J discussed in the introduction, the final g_J of 5S_2 oxygen is

$$g_J(^5S_2, ^{16}O) = \mu_J/J = -2.002\,091\,0(10).$$

This value and the 0.5 ppm quoted error cover about 82% of the measurements shown in the histogram in Fig. 6.

The measurement which has been described here is the first precision determination of the g_J factor of the 5S_2 metastable state of atomic oxygen. No

accurate theoretical computations have been published with which the measurement may be compared. However, after preliminary results were obtained,¹⁸ Hegstrom, using an approximate but simple computation which works well for 3S_1 He, found that the same procedure predicts the 5S_2 oxygen g_J to within 10 ppm.¹⁹

The combination of time-of-flight detection with an atomic-beam magnetic-resonance apparatus proved to be a sensitive technique for separating a particular discharge fragment from photons or other species affecting the beam detector. Additionally, the method allows limited control of the magnetic-resonance linewidth by selecting the velocity interval detected.

ACKNOWLEDGMENTS

We thank Peter J. Mohr, Michael H. Prior, and Charles Schwartz for their helpful counsel on the possible contributions of quadratic Zeeman shifts in helium and oxygen. One of the authors (T.I.) appreciates the hospitality of the Atomic Beam Group, Department of Physics and Lawrence Berkeley Laboratory of the University of California. He acknowledges the assistance of a grant from UNESCO. This research was supported in 1974 by the U. S. Atomic Energy Commission. The research group is now part of the Division of Chemical Science, Office of Basic Energy Sciences of the U. S. Department of Energy.

*Present address: Physics Dept., Middle East Technical University, Ankara, Turkey.

†Present address: Physics Dept., University of Missouri, Rolla, Missouri 65401.

¹R. S. Freund, J. Chem. Phys. 54, 3125 (1971); C. E. Moore, *Atomic Energy Levels*, U.S. Natl. Bur. Stand. Circ. No. 467 (U.S. GPO, Washington, D.C., 1949), Vol. 1.

²C. E. Johnson, Phys. Rev. A 5, 2688 (1972).

³W. C. Wells and E. C. Zipf, Phys. Rev. A 9, 568 (1974).

⁴G. Novak, W. L. Borst, and J. Fricke, Phys. Rev. A 17, 1921 (1978).

⁵C. A. Nicolaidis, Chem. Phys. Lett. 17, 436 (1972).

⁶C. C. Kiess and G. E. Shortley, J. Res. Natl. Bur. Stand. 42, 183 (1949).

⁷G. O. Brink, J. Chem. Phys. 46, 4531 (1967).

⁸E. Aygün, B. D. Zak, and H. A. Shugart, Phys. Rev. Lett. 31, 803 (1973).

⁹G. M. Keiser, H. G. Robinson, and C. E. Johnson, Phys. Rev. Lett. 35, 1223 (1975).

¹⁰B. E. Zundell and V. W. Hughes, Phys. Lett. 59A, 381

(1976).

¹¹R. H. Garstang, Rep. Prog. Phys. 40, 105 (1977).

¹²Tuncay Incesu, Ph.D. thesis (Middle East Technical University, Ankara, Turkey) (unpublished); also Lawrence Berkeley Laboratory Report No. 3351, 1974 (unpublished).

¹³P. A. Vanden Bout, V. J. Ehlers, W. A. Nierenberg, and H. A. Shugart, Phys. Rev. 158, 1078 (1967).

¹⁴M. P. Klein and D. E. Phelps, Rev. Sci. Instrum. 38, 1545 (1967).

¹⁵W. A. Anderson, Rev. Sci. Instrum. 32, 241 (1961).

¹⁶P. A. Vanden Bout, E. Aygün, V. J. Ehlers, T. Incesu, A. Saplakoglu, and H. A. Shugart, Phys. Rev. 165, 88 (1968).

¹⁷K. D. Böklen, Z. Phys. 270, 187 (1974).

¹⁸T. Incesu, A. Hug, and H. A. Shugart, in Fourth International Conference on Atomic Physics, Heidelberg, Abstracts, 1974 (unpublished), p. 231; also Bull. Am. Phys. Soc. 19, 1177 (1974).

¹⁹R. A. Hegstrom (private communication).